

**Science Requirements for SAMPAN :
The Satellite for Analyzing Microwave Polarisation Anisotropies**

François R. Bouchet, Martin Bucher, François-Xavier Désert,
Michel Piat, Nicolas Ponthieu, Michel Rouzé - 14/03/2006

SAMPAN is a space mission to carry out a full sky survey at high sensitivity of the CMB polarization with the aim of detecting primordial gravity waves generated during inflation. It will explore the best window available to probe new physics near the Planck scale.

The ESA PLANCK mission will provide a full sky survey accurately establishing the TT, TE, and EE correlations of the temperature and polarization of the CMB anisotropies with measurements limited only by cosmic variance up to approximately $\ell \simeq 1400$ (TT) and 500 (EE). PLANCK will allow the scalar perturbations to be characterized over three decades in wave number, and its measurement of the E-mode polarization will provide important cross checks. PLANCK, however, is not well suited for measuring the B-mode polarization anisotropy, which is the signature of gravity waves generated during inflation. With the reionization optical depth of $\tau = 0.17$ indicated by WMAP, PLANCK will be able to detect at 3σ a tensor-to-scalar ratio as small as $r \equiv (T/S) \approx 1.6 \times 10^{-2}$ using only the lowest multipoles ($\ell \lesssim 10$) to capitalize on the strong (factor $\approx 10^2$) enhancement of the tensor B-mode signal on the largest angular scales due to reionization. However, in practice it might prove difficult to distinguish a signal at such small ℓ from an explanation based on galactic foregrounds. On smaller angular scales, beyond this reionization induced peak at ($\ell \lesssim 10$), almost all the available signal-to-noise for detecting the primordial gravity wave B-polarization is concentrated over multipoles centered at around $\ell = 50$. In this range, PLANCK can directly detect only primordial signals larger than $(T/S) \approx 0.25$. On smaller angular scales ($\ell \gtrsim 200$) a background of E-polarization from scalar perturbations gravitationally lensed into the B-mode polarization dominates over the B-polarization signal arising from the tensor perturbations. Consequently, ground-based surveys, able to sample only a rather limited portion of the sky, cannot but marginally access the large scales where most of the information lies and therefore are not well-suited for measuring the B-mode primordial gravity wave signal, despite their potentially very high sensitivity.

The direct detection of primordial gravity waves, predicted by a broad class of inflationary models, would constitute a major breakthrough in our understanding of the physics near the Planck scale responsible for inflation. A single statistically significant detection of primordial gravity waves would establish the height of the inflationary potential. The height of the potential enters as an integration constant in the reconstruction of the gravitational potential from the inflationary scalar fluctuations. A more statistically significant detection allowing the primordial gravity wave power to be established at several wave numbers would allow one to test inflation by verifying the consistency relation predicted by inflation between the scalar and gravity wave power spectra characteristics. Other science benefits from SAMPAN include a clean characterization of the $EE \rightarrow BB$ gravitational lensing contaminant over the high- ℓ portion of the range accessible to SAMPAN, which promises to provide quite valuable information about the structures in place at around $z \approx 2$ and to provide new constraints on the nature of the dark energy.

The SAMPAN mission proposed here would be capable of detecting tensor-to-scalar ratios as low as $(T/S) \approx 1.5 \times 10^{-4}$ at the 3σ level using the reionization enhancement at the very lowest multipoles and (T/S) of approximately 2×10^{-3} with the information centered at around $\ell \approx 50$. Because the bulk of the available information in both cases is concentrated on large angular scales, a rather coarse angular resolution of the CMB anisotropy map of around 30 minutes of arc will suffice. The bulk of the improvement in sensitivity over PLANCK will result from the use of large bolometer arrays, reducing the effective detector noise from approximately $80 \mu\text{K} \cdot \text{arcmin}$ (sensitivity goal at 143 GHz) to approximately $5 \mu\text{K} \cdot \text{arcmin}$.

1 Brief history and present status of CMB observations

The measurements of the temperature and polarization anisotropies of the 2.7K cosmic microwave background (CMB) radiation provides a snapshot of the Universe at redshift $z \approx 1100$, only some 370,000 years after the Big Bang. Because of the small amplitude of the primordial anisotropies—of order 1 part in 100,000—the physics of the CMB is linear, allowing a clean and direct link to be established between the CMB observations and models for the possible new physics responsible for the generation of the primordial fluctuations at much earlier times. While observations of the structures in the universe at later times can also be used to measure the primordial fluctuations in a complementary range of smaller scales, the interpretation of these observations is complicated by the inherent nonlinearity of gravitational clustering at late times as well as by complicated intervening astrophysical processes.

The detection of the CMB by Penzias and Wilson in 1963 and the subsequent determination of the nearly perfect black body nature of its energy spectrum by COBE/FIRAS provided a solid observational confirmation of the hot Big Bang hypothesis. The competing steady state theory fell into disfavor because it was unable to provide a plausible explanation for the nearly exact Planckian nature of the CMB spectrum. The first measurement of the CMB anisotropy by the COBE space mission in 1992 established the overall normalization of the primordial fluctuations and also provided a loose constraint on the spectral index of the power spectrum, consistent with the nearly scale-invariant prediction from inflationary theory.

In the meantime, a host of ground and balloon based experiments have followed COBE, seeking to measure the CMB temperature anisotropy on smaller angular scales and with increased sensitivity as well as its polarization anisotropy. A series of experiments culminating with BOOMERANG firmly established the presence of the first acoustic peak at a multipole¹ $\ell \approx 220$, indicating the presence of plasma oscillations prior to decoupling. This observation led to the demise of topological defect models for the formation of structure. DASI provided the first measure of the EE polarization of the CMB, and a host of experiments leading up to the WMAP space mission provide an accurate mapping of the first few Doppler peaks. WMAP has measured the TE correlation and should announce its measurement for the EE correlation in its next data release.

The PLANCK satellite, to be launched in 2008, will extend the measurement of the TT correlations to smaller angular scales and will provide the first accurate characterization of the TE and EE spectra limited by cosmic variance up to $\ell \approx 1400$ and 500.

Presently, the CMB and other data available are consistent with a so-called “concordance” model characterized by a nearly scale-invariant spectrum of adiabatic scalar fluctuations with a logarithmic slope $n_s = 0.99$, a non-vanishing cosmological constant ($\Omega_\Lambda \approx 0.69$), a flat universe ($\Omega_k = 0$), a weakly interacting cold-dark matter component ($\Omega_{cdm} \approx 0.27$), and an abundance

¹The pattern of CMB anisotropies on the sky can be decomposed using a basis of spherical harmonics Y_ℓ^m , where the multipole ℓ corresponds to an angular scale $\sim 180^\circ/\ell$.

of baryons ($\Omega_b \approx 0.05$) consistent with primordial nucleosynthesis as well as a Hubble constant of $H_0 = 72 \text{ km s}^{-1} \text{ Mpc}^{-1}$. The optical depth to the last scattering surface has been determined by WMAP to be approximately $\tau \approx 0.17$. Future CMB data from WMAP and then PLANCK will offer increasingly stringent tests of this concordance model. It remains to be seen whether this agreement will persist with a more precise determination of the cosmological parameters of the “concordance” model or whether the new data will uncover anomalies indicative of new physics.

2 The Inflationary Paradigm : Scalar Cosmological Density Perturbations and Gravity Waves From Inflation

The present state of the observations, characterized by the so called concordance model described above, is consistent with a broad class of inflationary models. The idea of inflation was proposed in 1981 by Alan Guth to solve the monopole problem² and to explain why the universe is so nearly uniform on the largest scales as well as why it is so nearly spatially flat (i.e., why $\Omega_k = 0$ today). Guth’s initial proposal did not work, but very shortly thereafter Linde and Albrecht & Steinhardt in 1983 proposed a successful model of inflation, which may be described as “slow-roll” inflation. In this scenario, at early times the vacuum energy from a scalar field, called the “inflaton,” dominates the stress-energy of our Universe. Early on, the inflaton field, high on the potential, slowly “rolls” toward its minimum. The rapid expansion of the Universe introduces an effective friction term in the evolution equation governing the rolling of the inflaton field toward its minimum. During inflation, while this friction term dominates over the usual second time derivative term, the inflaton hardly rolls at all. Consequently, the potential energy of the inflaton dominates over its kinetic energy, giving rise to an equation of state very close to that of a cosmological constant. The temporary “cosmological constant” gives rise to a quasi-exponential evolution of the cosmological scale factor $a(t)$, hence the name “inflation.” Inflation ends with “re-heating,” when the inflaton field has rolled sufficiently far down the hill so that the second time derivative term dominates over the cosmological friction term, causing the inflaton field to roll more rapidly and decay by converting its energy into radiation.

During inflation, modes having a wave length initially within the “horizon” (or more accurately shorter than the Hubble length $H^{-1}(t)$)— that is, of physical wave number \mathbf{k} for which $|\mathbf{k}| \lesssim H_{inf}$ where H_{inf} is the Hubble constant during inflation—exit the horizon because of the exponential expansion, and their amplitudes become frozen in. After sufficient inflationary expansion, any perturbations that may have existed in the initial state prior to inflation have been swept out to scales far beyond the horizon and one is left with a virtually featureless

²One can show on very general grounds that one of the symmetry breaking transition from a unified theory at high energy to the low energy state of today lead to a copious production of magnetic monopoles, while none have ever been detected. Inflation is a means to dilute to unobservable densities these monopoles.

stretched vacuum. Such is the inflationary solution to the smoothness problem, and if it were not for quantum corrections, our universe would be too smooth to agree with the observations. After all, we do see galaxies and galaxy clusters on “small” scales, so at least some small primordial ripples are required to sow the seeds for the subsequent formation of these structures due to gravitational instability.

Fortunately, it was soon realized that the quantum fluctuations of the inflaton field provide small corrections to the completely uniform universe just described. Vacuum fluctuations of the inflaton field, initially hardly affected by the inflationary expansion, exit the horizon and become frozen in. These quantum fluctuations of the inflaton field advance or retard, depending on the sign of the fluctuation, the end of inflation and consequently transform into density perturbations at reheating. Because H_{inf} and presumably also the slope of the inflationary potential evolve very slowly as the inflaton rolls down the hill, the generation of these scalar perturbations is nearly self-similar. Perfect self-similarity would imply that $n_s = 1$ exactly (n_s stands for the logarithmic slope of the density power spectrum). Inflation consequently predicts a *nearly* scale invariant spectrum of scalar cosmological density perturbations.

By the same mechanism, gravity waves, or “tensor” perturbations, are also generated during inflation. Prior to their “horizon crossing” during inflation, the tensor modes, representing the gravitational wave degrees of freedom of the metric, fluctuate in much the same way as they would in flat Minkowski space. It is the value of the Planck constant \hbar that determines the amplitude of these quantum vacuum fluctuations. Let us follow the evolution of a single mode with co-moving wave number k (which would correspond to a physical wave number of (k/a) where a is the scale factor). As inflation proceeds, (k/a) increases, and because H during inflation remains roughly constant, eventually (k/a) becomes almost equal to H , corresponding to the “horizon crossing” of the mode k . As the mode crosses the horizon the single time derivative “cosmological friction” term in the evolution equation for the metric perturbation h^μ_ν (having a prefactor proportional to H) dominates over the second time derivative term, and the amplitude of the mode becomes frozen in at approximately its value at the moment of horizon crossing. As an order of magnitude estimate we have

$$h^\mu_\nu(k) \approx O(1) \left(\frac{H(k)}{M_{pl}} \right) \approx O(1) \left(\frac{V[\phi(k)]}{M_{pl}^4} \right)^{1/2} \quad (1)$$

where $H(k)$ is the value of the Hubble constant during inflation at the moment of horizon crossing of the mode of co-moving wave number k , M_{pl} is the Planck mass, $\phi(k)$ is the value the inflaton field when k crosses the horizon, and $V[\phi]$ is the inflaton potential. *Consequently, detecting the tensor spectrum $P_T(k)$ is roughly equivalent to measuring the height of the inflationary potential at the value of the inflaton field at the moment when the mode of wave number k exited the horizon.*

Following a similar line of reasoning, we obtain the following order of magnitude expression

for the spectrum of scalar density perturbations:

$$[P_S(k)]^{1/2} = \frac{\delta\rho}{\rho}(k) = O(1) \cdot \frac{V^{3/2}[\phi(k)]}{M_{pl}^3 V'[\phi(k)]}.$$

$P_S(k)$ therefore depends on both the height and the slope of the potential, while $P_T(k)$ is sensitive only to the height of the potential. A measurement of the latter therefore allows breaking the degeneracy between the two. The expressions for the scalar and tensor powers lead to the following consistency relation between the scalar and tensor power spectra characteristics³:

$$n_T = -\frac{1}{8} \left(\frac{T}{S} \right). \quad (2)$$

This relation is generic to all slow-roll models of inflation. Verifying this prediction would therefore provide a very strong, and unique, indication that inflation did actually take place. *Once the presence of tensor modes have been detected, the next most important goal is therefore to verify this relation, which requires reasonably precise measurements in a sufficiently broad range of angular scales.*

3 The CMB B Mode Polarization : A Signature of Primordial Gravity Waves

The primordial CMB polarization anisotropy manifests itself as temperature variations (always with the derivative of a black body spectrum) depending on the axis of the linear analyzer. The temperature in a given direction on the sky depends on the linear polarization according to $I + U \cos[2\phi] + V \sin[2\phi]$ where the angle ϕ indicates the orientation of the linear polarizer⁴. The magnitude of the polarization (i.e., $\sqrt{U^2 + V^2}$) and its orientation define a traceless tensor field on the celestial sphere, which may be thought of as a field of double-headed vectors. For comparing with theory, it is useful to decompose this traceless tensor field into two components: an E polarization component and a B polarization component. Here E and B refer to ‘electric’ and ‘magnetic’ type parity. The E polarization may be expressed as the second covariant derivative of a scalar potential Φ_E (with its trace removed) on the celestial sphere. The B polarization may be expressed as the second derivative of a pseudoscalar potential Φ_B with its trace removed followed by a rotation by 45° . The potential Φ_B is pseudoscalar rather than scalar because the choice of the sense of the 45° rotation entails a particular choice of handedness. Consequently Φ_B flips sign under spatial inversion (mirror image).

The distinction between the E and B polarizations is closely linked to the physics of underlying cosmological perturbations. In the linear theory, pure scalar modes (such as the fluctuations of the inflaton field responsible for the cosmological density perturbations) can produce only

³The scalar and tensor spectra powers P_S and P_T are taken to be ‘primordial’ and their normalization convention here coincides with that employed in the WMAP analysis papers and in the CAMB code. The tensor-to-scalar ratio is then $T/S \equiv P_T(k_0)/P_S(k_0)$ with $k_0 = 0.002 \text{ Mpc}^{-1}$.

⁴Circular polarization is not predicted within the standard cosmological framework.

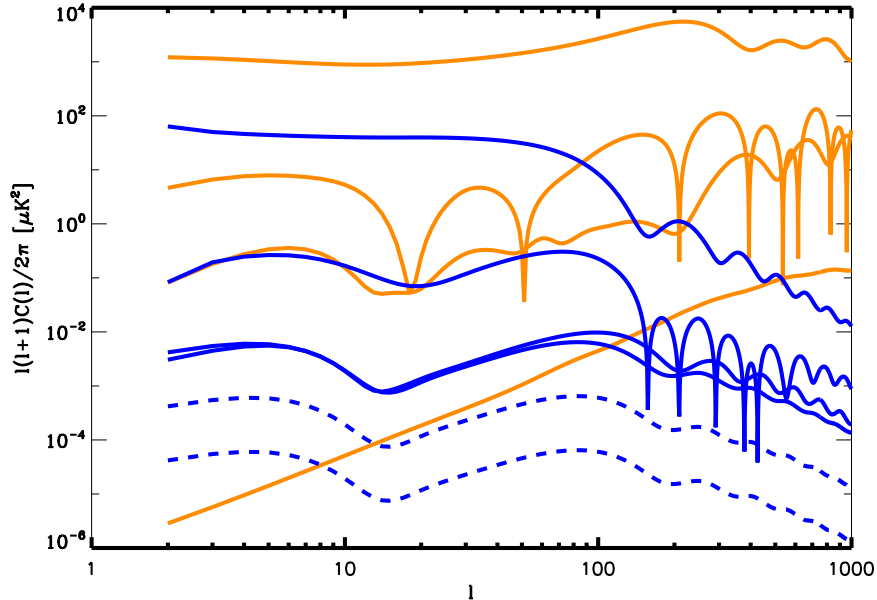


Figure 1: **Inflationary Prediction for the CMB Temperature and Polarization Anisotropies for the Scalar and Tensor Modes.** The red curves indicate the TT, TE, EE, and BB components (from top to bottom) generated by the scalar mode assuming ($H_0 = 72 \text{ km s}^{-1} \text{ Mpc}^{-1}$, $\Omega_b = 0.05$, $\Omega_{cdm} = 0.25$, $\Omega_\Lambda = 0.7$), no reionization, and $n_s = 0.99$ (an almost scale-invariant spectrum) are indicated by the red curves. The BB scalar component results from the gravitational lensing of the EE polarized CMB anisotropy at the last scattering surface $z \approx 1100$ by structures mainly around redshift $z \approx 2$. The horizontal axis indicates the multipole number ℓ and the vertical axis indicates $\ell(\ell + 1)c_\ell^{AB}/(2\pi)$ in units of $(\mu K)^2$, which is roughly equivalent to $dP^{AB}/d\ln[\ell]$. The TT, TE, EE, and BB (from top to bottom on the left) spectra resulting from tensor modes or primordial gravitational waves assuming a scale-invariant ($n_T = 0$) spectrum are indicated by the solid blue curves where it is assumed that the tensor-to-scalar ratio (T/S) is 0.1. The value corresponds roughly to the upper limit established by WMAP. The dashed lines indicate what the BB correlations would be for $r \equiv (T/S) = 0.01$ (top) and $r = 0.001$ (bottom), respectively. For the TE cross-correlations we have plotted the log of the absolute value, hence the downward spikes corresponding to the sign changes of this cross correlation.

E type polarization. By contrast, tensor modes may produce both *E* and *B* type polarization. *Consequently, the presence of B type polarization attributable neither to foreground contamination nor to nonlinear corrections is the telltale sign of the presence of primordial gravity waves.*

The most plausible scenario for generating primordial gravitational wave is inflation. As discussed above, inflation predicts the generation of gravitational waves, their amplitude proportional to the height of the inflationary potential when the relevant modes exit the horizon. Fig. 1 shows the CMB anisotropy for an inflationary model with its parameters chosen to agree with the concordance values taken from the WMAP analysis. The red curves indicate the anisotropies arising from the scalar mode and the solid blue curves indicate the tensor anisotropies with a tensor-to-scalar ratio of $(T/S) = 0.1$. From top to bottom on the right the blue curves indicate the TT, TE, EE and BB tensor anisotropies⁵, assuming a spectral index

⁵Angular power spectra can be defined as the harmonic transforms of a correlation function of two quantities. TT, EE and BB therefore refer to the spectra of the autocorrelation function of (respectively) the T, E, and B patterns, while TE refers to the cross-correlation between the T and E fields.

of $n_T = 0$, which is the inflationary prediction when (T/S) is negligibly small. For the BB spectrum, the shape predicted for $(T/S) = 0.01$ and 0.001 , obtained simply by a downward translation on the logarithmic scale, is indicated by the blue dashed curves. The red scalar curves (from top to bottom on the left) correspond to the spectra for the TT, TE, EE and BB (from lensing) anisotropies arising from the scalar mode. In the absence of nonlinear corrections the scalar BB signal would be exactly zero. However, a contaminant signal arises from the gravitational lensing of E -polarization on the last scattering surface (at $z \approx 1100$) by clustered matter lying between $z \approx 1100$ and $z = 0$. Such lensing, primarily due to structures present at around $z \approx 2$, creates distortions, which turn E -polarization into B -polarization from the perspective of an observer at $z = 0$.

Fortunately, this background of scalar B polarization is calculable and has a spectrum peaking at large ℓ . For a given set of cosmological parameters, the standard Boltzman solvers such as CMBFAST and CAMB calculate the BB lensed scalar power spectrum $c_\ell^{BB, lens scal}$. Other cross checks are available such as measuring the lensing potential of the CMB directly using higher order correlation functions of the CMB having a vanishing expectation value in a Gaussian theory. In Fig. 1 we observe that for intermediate ℓ lying roughly in the range 15–70, the signal $c_\ell^{BB, tens}$ and contaminant $c_\ell^{BB, lens scal}$ spectra have roughly the same shape and are of roughly equal magnitude for $(T/S) \approx 0.01$. The enhancement on larger angular scales ($\ell \lesssim 15$) is entirely due to the reionization present in the model, where the optical depth $\tau = 0.17$ from WMAP has been assumed. Under the hypothesis of no reionization, the roughly white noise spectrum of $c_\ell^{BB, tens}$ over the range 15–70 would extend down to $\ell = 2$. Beyond $\ell = 70$ the lensing contribution becomes dominant.

Here we have described the inflationary prediction for the B modes as well as the character of the lensed contaminant. The direct discovery of primordial tensor modes would revolutionize our understanding of the early universe because:

(1) A measurement of the B mode spectrum would allow the reconstruction of the inflationary potential over a finite range and provide important clues for superstring model builders seeking to explain the origin of the inflationary potential within the framework of fundamental physics.

(2) While more difficult, a verification of the consistency relation in eqn. (2) would at last provide a stringent test of the inflationary paradigm. If established with sufficient precision, one may forecast that inflation would then become the finishing piece in the standard model of cosmology.

4 Other candidate sources of primordial B modes

Given that simple single-field inflationary models (or more precisely a broad range of such models) are capable of providing a theoretical foundation for the concordance model, it is

logical to consider gravitational waves from inflation as the most likely candidate for generating primordial B modes. Nevertheless other candidate mechanisms exist and constitute the subject of this subsection.

Moreover, galactic and other foreground contaminants because of the nonlinearity of their underlying physical mechanisms, predict E and B polarization in roughly equal proportions. For this reason, broad frequency coverage for effective component separation and coverage of the galactic plane, to characterize the polarization properties of the foregrounds will be necessary for separating out the primordial signal.

The argument that scalar modes from inflation cannot generate any B mode relies crucially on the linearity of inflation. Primordial B modes are not possible as long as the relevant underlying degrees of freedom may be described by a scalar order parameter field and higher order effects are negligible. These conditions are clearly satisfied for the case for single-field inflation (where, for example, for a $\lambda\phi^4$ potential, $\lambda \approx 10^{-12}$ is required in order to obtain cosmological density perturbations of the right amplitude to agree with the observations). However, multi-field models have been proposed exhibiting appreciable nonlinearity, which in principle could generate a measurable B mode polarization in the CMB.

Topological defects in the early universe constitute another candidate for the generation of primordial B mode polarization in the CMB. Prior to the observation of the first Doppler peak by the BOOMERANG balloon-borne CMB probe, topological defect based scenarios for structure formation contended with inflationary models. However, the presence of a well-defined Doppler peaks ruled out these scenarios as the sole or primary source of cosmological density perturbations. It nevertheless remains possible that less massive topological defects may contribute sub-dominantly to the cosmological perturbations. Such defects, because of their highly non-linear evolution, are expected to excite E and B modes in roughly equal proportions.

If B modes are observed, the two alternative scenarios may be distinguished from B modes from gravity waves generated during inflation by their non-Gaussianity. *Indications for any of these or other unexpected sources of primordial B modes would constitute a major discovery which is likely to provide even more insight into the physics near the Planck scale.*

5 Detecting Primordial Gravity Waves with SAMPAN

Having discussed the primordial gravity waves from inflation expected from the concordance model as a function of the unknown scalar-to-tensor ratio (T/S), we now examine their detectability. At all scales over which the primordial B modes may be detectable ($\ell \lesssim 100$), the spectrum from E lensing has a white noise shape, with a normalization close to $5 \mu\text{K} \cdot \text{arcmin}$. The meaning of that normalization is that the rms of the corresponding noise would be $5/\theta \mu\text{K}$

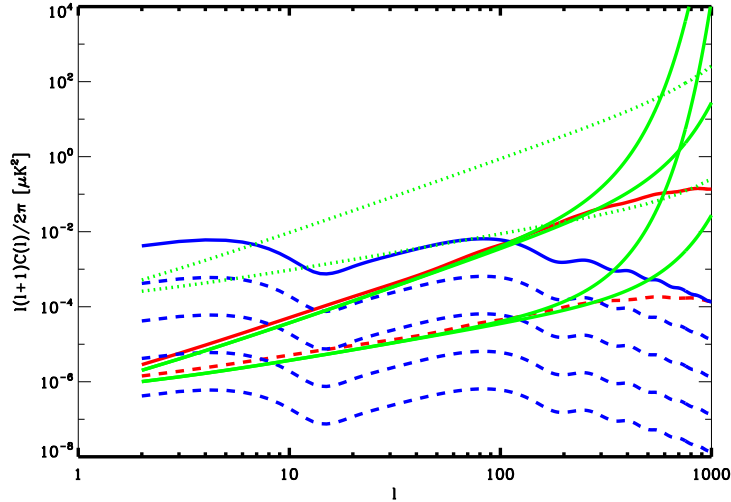


Figure 2: Relative sensitivities of PLANCK and of SAMPAN versus B modes, assuming for the latter $5\mu\text{K} \cdot \text{arcmin}$ instrument noise and either $20'$ or $40'$ fwhm beams. Planck corresponds to the dotted green lines and SAMPAN to the solid ones. In each case, we plot both the expected detector noise power spectrum, and its division by ℓ to suggest the detection achievable in broad bins ($\Delta\ell/\ell \sim 1$). From top to bottom, the B modes levels in blue correspond to values of $(T/S) = 10^{-1}, 10^{-2}, 10^{-3}, 10^{-4}, 10^{-5}$.

in a square pixel of θ arcmin on each side. A detector noise contribution in the E and B maps⁶ at that level of $5\mu\text{K} \cdot \text{arcmin}$ is the sensitivity goal of SAMPAN.

Fig. 2 shows the sensitivities of PLANCK and of SAMPAN for two different beam widths in relation to the primordial tensor BB signals for $(T/S) = 0.1, 0.01, 0.001$ and the background BB lensed scalar contaminant. The upper dotted green curve indicates the instrument noise of PLANCK,⁷ enhanced by a factor of $\exp[+(\ell\sigma_{bw})^2]$ on small angular scales to account for the attenuation of the signal due to smearing by the finite width beam profile. The lower dotted curve divides this noise by ℓ to provide an estimate of how much the sensitivity can be increased through broad binning (i.e., broadband filtering where $(\Delta\ell)/\ell \approx 1$). We observe that PLANCK has little chance of making a primordial B mode detection except over the range $\ell \lesssim 15$ due to the enhancement of the unlensed tensor signal from reionization. On these very large angular scales (i.e., $\ell \lesssim 15$), assuming the best-fit WMAP reionization optical depth $\tau = 0.17$, the BB signal is enhanced by a factor of (≈ 100). This enhancement may be understood qualitatively as follows.

On very large angular scales, the polarization is roughly proportional to the double gradient of the velocity field multiplied by the square of the distance between last and next-to-last scattering. Here we assume that over the distances in question the Taylor expansion to second order is sufficiently accurate. In the absence of reionization, the relevant distance is the thickness

⁶Or equivalently of the Q and U maps.

⁷At 100, 143 and 217 GHz, Planck has a Q and U sensitivity goal of 100, 80, and $135\mu\text{K} \cdot \text{arcmin}$, respectively, (with corresponding angular resolutions of 9.5, 7.1 and 5 arcmin FWHM). Here we illustrate Planck sensitivity by assuming that the CMB maps resulting from the astrophysical component separation procedure will be akin to the properties of the 143 GHz channel map and have a resolution of 7.1 arcmin FWHM and a detector noise amplitude of $80\mu\text{K} \cdot \text{arcmin}$.

of the last scattering surface. However, for the contribution from reionization, the relevant distance is much larger, than traveled by a light ray between $z \approx 1100$ and z_{reion} . When the wave length of the mode is shorter than or of the same order as this distance, this second derivative approximation is no longer valid, and there is instead an attenuation due to smearing, hence the precipitous drop around $\ell \approx 10$. While reionization provides a remarkable amplification of the BB tensor signal for very low ℓ , it could in practice turn out difficult to rule out a galactic foreground explanation for this signal. Consequently, a conservative analysis would mainly rely on the signal at larger ℓ , where the signal can be separated into high and lower galactic latitude components. We therefore try to present separately the limits obtained with and without this reionization enhancement.

(T/S)	$2 < \ell < 15$	$16 < \ell < 100$	$101 < \ell < 200$
PLANCK	1.6×10^{-2}	0.25	1.0
SAMPAN	1.5×10^{-4}	2.2×10^{-3}	8.8×10^{-3}
Cosmic variance	8.6×10^{-5}	1.2×10^{-3}	5.0×10^{-3}

Table 1: Thresholds for a 3σ detection of primordial gravity waves with PLANCK, SAMPAN and an ideal cosmic variance limited full-sky polarization survey.

Table 1 indicates the 3σ (T/S) detection thresholds for PLANCK, SAMPAN and an ideal cosmic variance limited experiment having vanishing instrument noise. In the latter case, only the finite number of modes measurable on the sphere limits the possible inference on the theory. Here we assume a noise variance of 6400 and 25 $(\mu\text{K} \cdot \text{arcmin})^2$ for PLANCK and SAMPAN, respectively, and uniform beam widths of 10 arcmin FWHM. It is assumed that all the other cosmological parameters are known, so that there is no uncertainty in the underlying power spectrum of the lensed $E \rightarrow B$ scalar contaminant. The ideal experiment on the last line is subject only to noise due to the cosmic variance of the lensed $E \rightarrow B$ scalar contaminant. The χ^2 for distinguishing the tensor B-mode signal of a power characterized by (T/S) from the detector noise and lensed contaminant signal is given by multiplying the sum below by $(T/S)^2$:

$$\frac{\chi^2}{(T/S)^2} = \sum_{\ell} f_{sky} \frac{(2\ell + 1)}{2(c_{\ell}^{BB, lens scal} + n_l \exp [+(\sigma_{bw}\ell)^2])^2} \left(\frac{\partial c_{\ell}^{BB, tens}}{\partial (T/S)} \right)^2 \quad (3)$$

We divide this sum over multipoles into three bins for ℓ : [2, 15], [16, 100], and [101, 200]. The first bin contains almost all the enhancement due to reionization. The second bin contains almost no reionization enhanced signal and most of the signal that would be present for $\tau = 0$. The third bin is provided to illustrate that little additional information is to be gained beyond $\ell \approx 100$.

Fig. 3 gives an idea, through another means, of where (at which multipoles) the pertinent information lies. The contribution to χ^2 at a given multipole is given by

$$\frac{\chi^2}{(T/S)^2} = f_{sky} \frac{(2\ell + 1)}{2(c_{\ell}^{BB, lens scal} + n_l \exp [+(\sigma_{bw}\ell)^2])^2} \left(\frac{\partial c_{\ell}^{BB, tens}}{\partial (T/S)} \right)^2 \quad (4)$$

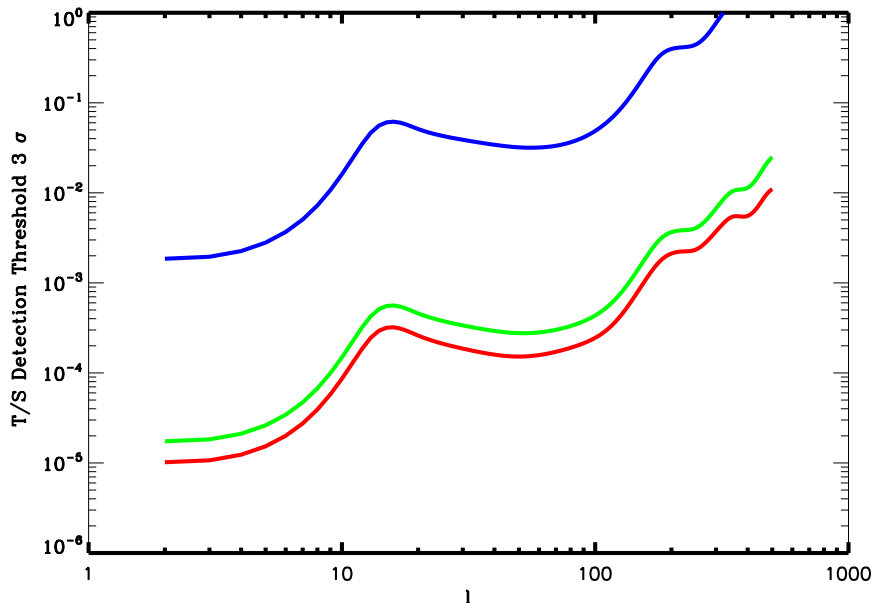


Figure 3: **Where does the information lie?** To give a rough idea of the angular scales where the information lies, we assume a broad binning, with $\Delta\ell \approx \ell$, and plot three times the reciprocal of ℓ times $\chi^2(\ell)/r^2$, which is roughly the threshold for a 3σ detection using the information broadly centered at ℓ . From top to bottom the curves correspond to Planck, SAMPAN, and an ideal noiseless experiment.

Taking three times the reciprocal of the square root of ℓ times the quantity of the right hand side of eqn. (4) gives roughly the threshold for a 3σ detection of nonvanishing (T/S) resulting from broadband binning, with $(\Delta\ell) \approx \ell$. It is worth noting how close SAMPAN gets to what can be achieved by an ideal noiseless experiment⁸.

All the above analyses have assumed that all the scalar cosmological parameters are completely known. To get an idea of how much the uncertainties in the cosmological parameters, and hence in the spectrum of the lensed $E \rightarrow B$ scalar contaminant, might degrade the detection threshold for (T/S) , we perform a Fisher matrix analysis⁹, constructing a linear parametric model with eight parameters including (T/S) . A fiducial model without reionization is assumed. As can be seen from the results in Table 2, the 3σ thresholds are not significantly degraded. We obtain for a 20 arc minute beam a 3σ detection for $(T/S) > 3 \times 6.60 \times 10^{-4} \approx 2 \times 10^{-3}$ which does not rely on the low- ℓ reionization bump (since the fiducial model assumes $\tau = 0$).

Fig. 4 illustrates the effect of the angular resolution of the CMB mapping on the primordial tensor mode detection threshold. The plot indicates that the best detection capability is reached for a resolution of about 40 arc minutes, with a rather quickly increasing degradation for lower

⁸In such a case though, we could envisage using the noiseless maps of the T and E anisotropies to predict and remove very accurately the B contribution arising from lensing. Preliminary analyses indicate that one would then need rather very high angular resolution and sensitivity, of the order of $1\mu\text{K} \cdot \text{arcmin}$ for a resolution better than 3 minutes of arc, i.e. probably a cornerstone class mission

⁹A Fisher matrix analysis relies on a multivariate approximation of the likelihood of the data given an underlying (fiducial) model. While this approximation cannot do justice to exact shape of the likelihood function describing the data, especially in the tails of the distribution, it does provide sufficient guidance for an early design phase.

	Fiducial model	SAMPAN 20' fwhm, $(5\mu\text{K} \cdot \text{arcmin})^2$ (No reionization)					
		TT	TE	EE	BB	BB+EE	All
r	0.0	1.57×10^{-1}	7.19×10^{-2}	1.32×10^{-2}	1.58×10^{-3}	6.71×10^{-4}	6.60×10^{-4}
$\delta A_S/A_S$	1.00×10^0	3.14×10^{-1}	6.15×10^{-3}	3.81×10^{-3}	2.70×10^0	3.57×10^{-3}	1.27×10^{-3}
H	7.20×10^1	9.96×10^{-2}	6.62×10^{-2}	9.91×10^{-2}	5.94×10^0	8.06×10^{-2}	3.93×10^{-2}
Ω_b	5.00×10^{-2}	3.43×10^{-4}	2.68×10^{-4}	6.01×10^{-4}	3.91×10^{-2}	4.88×10^{-4}	1.39×10^{-4}
Ω_c	2.50×10^{-1}	3.73×10^{-5}	5.03×10^{-5}	1.34×10^{-4}	3.45×10^{-2}	1.28×10^{-4}	2.68×10^{-5}
n_s	1.00×10^0	3.47×10^{-3}	6.69×10^{-3}	3.98×10^{-3}	1.49×10^{-1}	3.74×10^{-3}	1.84×10^{-3}
Ω_k	0.0	5.53×10^{-4}	4.37×10^{-4}	3.08×10^{-4}	3.04×10^{-2}	3.01×10^{-4}	1.87×10^{-4}
τ	0.0	1.73×10^{-1}	8.00×10^{-4}	1.19×10^{-5}	1.60×10^0	5.96×10^{-6}	5.96×10^{-6}

Table 2: 1σ errors resulting from the fit of an eight parameter family of cosmological models for a detector rms white noise amplitude of $5\mu\text{K} \cdot \text{arcmin}$ and a resolution of 20 arc minute. (Note that $\delta A_S/A_S$ denotes the variation of the normalization of the scalar power spectrum as compared to that inferred from COBE data.) This table confirms that a tensor-to-scalar ratio (T/S) greater than 2×10^{-3} could be detected at the 3σ level even without relying on the low- ℓ reionization bump.

angular resolution. *We therefore set as a scientific requirement for the study that all channels contributing to the CMB mapping would have a resolution at least as good as 40 arcminutes, with a goal to achieve twice better.*¹⁰

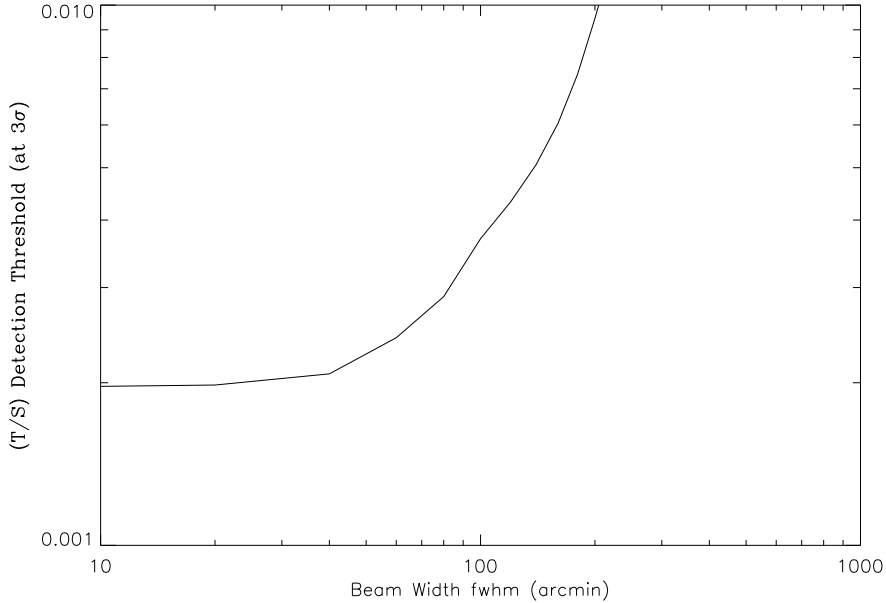


Figure 4: **Effect of angular resolution.** The curves illustrate the variation of the 3σ limit on r which can be derived from a Fisher analysis as a function of the postulated angular resolution (in arc minutes fwhm), for the same sensitivity of $5\mu\text{K} \cdot \text{arcmin}$.

¹⁰An improved angular resolution would additionally much improve SAMPAN capabilities for other scientific endeavours, e.g., determining the matter power spectrum, although a numerical assessment of the latter remains to be done.

Further reading: “US Task force report on Cosmic Microwave Background Research”, which may be downloaded at www.science.doe.gov/hep/TFCRreport.pdf

6 Payload requirements

6.1 Overall Requirements

The primary goal of the SAMPAN mission is the measurement of the B -modes of the CMB polarization with enough sensitivity to measure the imprint of the primordial gravitational wave background from GUT scale inflation. Equivalently, the sensitivity must be such that all B -modes created by gravitational lensing deformation of the E -modes are mapped at or close to the cosmic variance limit on large angular scales.

The scientific objective of SAMPAN requires that the payload instrument fulfill the following main requirements. Whenever possible we define a baseline requirement (BaseReq) as well as a minimum requirement (MinReq).

1. The frequency coverage must be broad enough to provide robust removal of the foregrounds. The CMB spectrum peaks in the millimeter domain. The best window for CMB measurements lies between 70 GHz and 217 GHz. One may view the emission on the sky as a superposition of the CMB with a number of contaminant foregrounds, each having its own spectral signature. The foreground removal essentially reduces to resolving a system of linear equations. Measurements at N frequencies allow one to isolate at most N components, or more safely $(N - 1)$ with some redundancy. An absolute minimum of four frequency bands are therefore needed to separate with some redundancy the CMB from the main low and high frequency contaminants. Adding at least one more channel would allow separating at least one further spectral contribution, which is highly desirable.

Bolometric cameras are currently the most sensitive technology available and operate nearly at the shot noise limit. This technology, however, is currently unproven at frequencies below 100 GHz. The Baseline Requirement therefore specifies four spectral bands centered about 100, 143, 217, and 353 GHz. This choice enables measurement at frequencies close to the minimum of the foregrounds at low (100 GHz) and at the minimum, null, and maximum of the Sunyaev-Zeldovich effect (143, 217, 353, GHz). All these frequencies are common with Planck to enable instrument calibration cross-checks. This frequency range would be complemented by two additional optional channels on both sides, at 70 GHz to better monitor the free-free and synchrotron emission and at 545 GHz to better monitor the dust emission and the unresolved infrared galaxy background. Since we seek to probe a continuous spectrum, a low frequency resolution of $\Delta\lambda/\lambda \approx 0.35$ suffices.

2. The sensitivity must be sufficient for adequate detection of the different polarization

modes of the CMB. The level of the B modes induced by lensing deformation of the E modes is predicted at the $5 \mu\text{K} \cdot \text{arcmin}$ level on all scales larger than a fraction of a degree. The target CMB B-mode sensitivity is therefore $5 \mu\text{K} \cdot \text{arcmin}$, and it should be no worse than $7 \mu\text{K} \cdot \text{arcmin}$. Here we make the conservative assumption that we could not benefit from a square root of two improvement from the joint use of the two adjacent CMB channels. Consequently, the sensitivity to the Stokes parameters Q and U (equivalent to the E and B sensitivities if the sky coverage f_{sky} is close to 1) would be the following. For each of the central frequency bands (143 and 217 GHz), the BaseReq is $5 \mu\text{K} \cdot \text{arcmin}$ and the MinReq is $7 \mu\text{K} \cdot \text{arcmin}$.

For the 100 GHz channel, we require the same than at 143 GHz, and decrease the requirement by a factor of two for the optional 70 GHz channel. The requirement for the 350 GHz is three time worse than at 217GHz, while it is ten times worse for the optional 545 GHz channel. This is summarized in Table 3. In any case, this apportioning is only indicative in order to determine the instrumental needs. Once more information on polarised foregrounds becomes available, optimization studies can then see how to best use the available focal plane space and power.

As a simple formula, the noise in the power spectrum (excluding cosmic variance) for a single multipole is :

$$\Delta C_\ell = \left[\frac{2}{(2\ell + 1)f_{sky}} \right]^{1/2} \times C_{noise} \exp \left[\ell^2 \left(\frac{FWHM}{2.35} \right)^2 \right] \quad (5)$$

where $C_{noise} = 8\pi f_{sky} s_{det}^2 / (N_{det} T_{mission})$ where s_{det} is the detector I sensitivity in $\mu\text{K} \cdot \text{s}^{1/2}$, N_{det} is the number of detectors, f_{sky} is the fraction of the sky surveyed, $T_{mission}$ is the total survey time in seconds, and FWHM is the beam full width at half maximum in radians. The factor of two accounts for the polarization measurement efficiency. Fig. 5 illustrates the error bars after binning attainable with the baseline SAMPAN specification (of approximately $15^2 = 225$ times better noise variance compared to Planck). This would enable SAMPAN to detect at 3σ a tensor-to-scalar ratio above $T/S \simeq 2 \times 10^{-3}$ (corresponding to an inflationary energy scale of 7×10^{15} GeV).

3. The angular resolution must be of order $10'$ ($20'$ as a MinReq) at the frequencies where the CMB signal is dominant, which we take here to include all frequencies greater than 100 GHz.

More precisely, the angular resolution as BaseReq, given as the full-width at half maximum (FWHM) in arcminutes would be diffraction limited below 217 GHz, $10'$ at 217 GHz and above ($22'$ at 100 GHz and $10'$ at 353 GHz).

The MinReq would be $20'$ at 217GHz and above and at the diffraction limit below 217 GHz. See Table 3 for a summary.

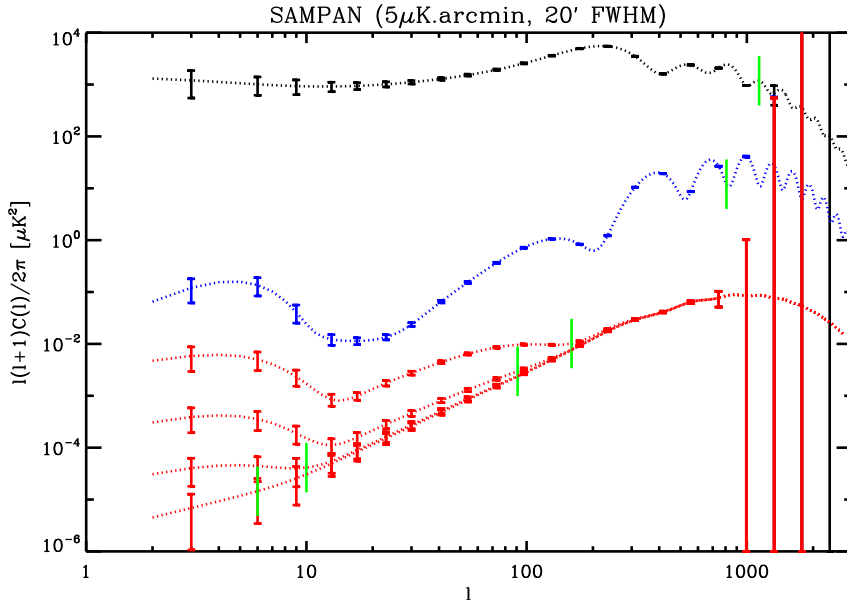


Figure 5: Illustration of the attainable error bars (including cosmic variance) on the (binned) power spectra for the temperature anisotropies (top, black), the E -modes (blue, middle) and the B -modes with $T/S = 10^{-1}, 10^{-2}, 10^{-3}, 10^{-4}$ corresponding, respectively, to the red dotted lines from top to bottom. In the latter case, the spectrum is virtually indistinguishable from that induced by lensing only. The green ticks delimit the low- l region where the measurement would not be limited by detector noise (assuming $f_{sky} = 0.8$).

6.2 Payload Requirements

To achieve the scientific objectives outlined in sections 5 and 6.1, the model payload imposes a number of requirements on the mission, which in turn determine an appropriate observing strategy (see 2 below):

1. As mentioned earlier, SAMPAN aims to measuring the primordial gravitational wave background. An essential feature of its imprint on the CMB polarization is the bump at large angular scales (induced by an early reionization). In order to best detect this power, one must cover a large fraction of the sky (f_{sky}) to overcome cosmic variance (the cosmic variance scales as $1/f_{sky}$). The need for large sky coverage and coverage of large

					Option	
Central Frequency (GHz)	100	143	217	353	70	545
Bandwidth ($\Delta\nu/\nu$)	0.35	0.35	0.35	0.35	0.35	0.35
Angular Res. (FWHM, arcmin) - Reqs	40	30	20	20	60	20
Angular Res. (FWHM, arcmin) - Goal	20	15	10	10	30	10
Q & U Sensitivity ($\mu\text{K} \cdot \text{arcmin}$) - Reqs	7	7	7	20	15	200
Q & U Sensitivity ($\mu\text{K} \cdot \text{arcmin}$) - Goal	5	5	5	15	10	150

Table 3: Characteristics and sensitivity of the SAMPAN frequency channels. Note that all channels are diffraction limited at frequencies below 217 GHz.

angular scales constitutes a formidable limitation for ground based and balloon borne experiments. In order to maximize the return, we require a full sky survey, and estimate that 80 % sky coverage will be available for CMB analysis once a sky selection has been performed (during data analysis to limit foreground contamination where it is strongest, in particular close to the Galactic plane).

2. The **observing pattern** must be periodically repetitive to enable adequate control of systematic instrumental effects such as baseline and gain drifts. Periodicity over longer time scales (monthly, yearly) is also necessary for jack-knife consistency tests. We have set for this study the following requirements on the scan strategy:

- (a) At least 4 all-sky surveys must be performed to test for data reproducibility. Due to Sun-Earth-Moon constraints this implies a survey duration of at least 2 years. Every 1 to 3 days approximately half the sky must be observed with a maximum of redundancy and of polarizer orientations. The Baseline Requirement is that a given detector must observe several times some (the more the better) pixels with a time lag of at most 5-10 seconds (10-20 for Minimum Requirement) and with a different polarizer orientation (The angle must be at least 15 degrees and ideally 90 degrees). All pixels must have been observed with at least 3 orientations to enable the reconstruction of I , Q and U .
- (b) Over a period of 10 minutes, polarization measurements have to be correlated between regions separated by at least 40 degrees (a constraint set in order to help measure accurately low multipoles of the spherical harmonic expansion).
- (c) The sky coverage must be as homogeneous as possible. Although difficult to specify at this stage, homogeneity will be a criterion to choose among competing scanning strategies fulfilling the above requirements. Some deeply integrated regions, however, may also provide valuable information for cross calibration and systematics monitoring.

The above choice of time scales for redundancy is based on an anticipated knee frequency¹¹ (~ 100 s) of the detector chain and assuming, as confirmed by experience, that the knee frequency can be taken to be about 10 times lower for differenced quantities.

3. **Systematic effects** must be kept under a level such that they do not limit the accuracy of the observations, which should be dominated by the instrumental sensitivity. The main sources of spurious signal are gain drifts, stray light, thermal variations, and

¹¹The knee frequency is the threshold below which the detector noise starts exceed the white noise extrapolation from higher frequencies due to $(1/f)$ noise.

interference due to the TM/TC system. Since it is difficult at this stage to set individual requirements on each systematic, we impose the global requirement that the sum of systematic effects must be less than the instrumental noise, or that they can be determined (and thus subtracted) with an accuracy better than 1/10 of the instrumental noise.

4. **Satellite Orbit:** Parasitic signals from the Earth in far side lobes must be less than the on-beam sensitivity. A basic calculation shows that placement at the second Lagrangian point (L2 as for Planck) allows an optics with side lobe rejection of 10^{-9} instead of 10^{-14} for low Earth orbits where the Earth occupies almost a solid angle of 2π . It would seem that for polarization measurements, as we add one level of differentiation, we can relax this constraint. Actually, side lobes are likely to be polarized (from 5 to 50 %) so that the Earth, Sun and Moon can produce a parasitic polarized signal on the sky which is only slowly varying in time and hence can mimic a true polarized sky. The L2 orbit satisfies the side lobe rejection requirement as the Earth, Sun and Moon are kept at more than 70 degrees off the main beam. Spitzer-like orbit (trailing or leading the Earth on its orbit) can be considered (for telemetry reasons) but the constraint of an all-sky coverage while excluding the Moon is then quite difficult to satisfy.

5. **Absolute pointing** for the satellite: The satellite should point opposite to the Earth for the scientific telemetry downlink and avoid the Sun, Earth and Moon in the V -grooves which enable passive cooling. The absolute pointing, therefore, need not to be accurate to better than about a degree (for telemetry, cooling, and control of far side lobes, since for the science data, only the *a posteriori* reconstruction is important).

6. **Pointing reconstruction:** Only an *a posteriori* knowledge is needed. However it must be very accurate: a rms deviation of at most 1/20th of the diffraction spot (FWHM) for each of the 217 GHz detectors for the 3 axes. The third axis (roll angle) is important for the polarization measurements. The orientation of all detectors must be known with an accuracy better than (BaseReq) 0.075° (0.15° MinReq) for a duration equal to an integration time. Inaccuracies in the pointing reconstruction lead to an increase of the effective beam width. The intercomparison of the measurements by different bolometers becomes inaccurate. Therefore the final error in the final polarization power spectrum increases at large multipole number.

7. **Integration time and stability:** The satellite will not drift by more than 1/3 FWHM during one elementary integration time, typically 10ms.

8. **Maximum telemetry rate:** The scientific data compression rate will be from 16 (imposed by the dynamical range on the sky) to 4 bits per measurements (enough to characterize a mostly Gaussian noise).
9. **Orbital domain** forbidden by the mission: The only constraint is the instrumental telemetry.

6.3 Instrumental baseline

The effective instrument noise may be summarized by means of the following formula:

$$C_{noise} = (5\mu\text{K} \cdot \text{arcmin})^2 \times \left(\frac{2 \text{ years}}{T_{mission}}\right) \times \left(\frac{5000}{N_{det}}\right) \times \left(\frac{s_{det}}{140\mu\text{K} \text{ s}^{1/2}}\right)^2$$

The required detector sensitivity can be achieved for an overall instrumental efficiency of 0.3, an average of 6 detectors per diffraction beam and a total bolometer NEP (noise equivalent power) of typically $4 \times 10^{-18} \text{ W Hz}^{-1/2}$, close to background limited performance. We have assumed a typical sensitivity for 100 mK bolometer array. Details may be found in an accompanying Excel spreadsheet. It is important to bear in mind that the ambitious goal sensitivities in 4 bands leads to a rather large number of pixels (typically 20,000 for the 4 bands).

Such a large number of detectors has important implications for the instrument architecture, especially on the cryogenics and the telemetry rate. As shown in the following table, we have estimated the interfaces of the focal plane with the rest of the instrument with two different detector technology being developed in the DCMB collaboration: semi-conductor bolometers using JFETs as first amplifier stage and superconducting bolometers with SQUIDs readout.

The two kinds of detector technology lead to similar interfaces for the coldest stage and for the 300K electronics. The main difference arises at intermediate temperature due to the different readout scheme. The choice between the two technologies will therefore be made based on detector behavior, availability, and simplicity.

Focal plane components	Characteristics	20000 detectors SQUID (f=32)	20000 detectors JFET (f=16)
Detectors: Stage at 0.1 K or 0.3 K	Dimensions (diameter) Mass (Kg) Electrical Power (W) Number of wires	291 mm 3 $1. \times 10^{-6}$ 2600	291 mm 3 975×10^{-9} 2704
SiGe: Stage at $50 \text{ K} \geq T \geq 4 \text{ K}$	Dimensions Mass (kg) Electrical Power (W) Number of wires	$20 \times (110 \times 110 \times 40) \text{ mm}^3$ 7,8 156×10^{-3} 364	0 0 0 2704
JFET: Stage at $T < 150 \text{ K}$	Dimensions Mass (kg) Electrical Power (W) Number of wires	0 0 0 364	$40 \times (150 \times 150 \times 40) \text{ mm}^3$ 20,8 1,63 6032
Warm Amplifiers: Stage at 300 K	Dimensions Mass (Kg) Electrical Power (W) Data rate (Mbits/s)	$(400 \times 400 \times 400) \text{ mm}^3$ 25 < 200 W 5,7	$(400 \times 400 \times 400) \text{ mm}^3$ 25 < 200 W 5,7

Table 4: Instrumental requirements